Erasmus University Rotterdam
Erasmus School of Economics
Bachelor Thesis Econometrics and Operations Research

Assessing the Delay in Arctic Ice Loss through the Utilisation of Carbon Capture and Storage

Ece Hale Taskin (595810)

Supervisor:	D.J.W. Touw
Second assessor:	F. Frasincar
Date final version:	1st July 2024

Abstract

The Arctic environment, weather, and temperature may all suffer as a result of the recent sea ice changes, which also have significant implications for society and the economy. This analysis was a replication of (F. X. Diebold, Rudebusch, Göbel, Coulombe & Zhang, 2022), wherein linear carbon trends were used to project the arrival timings for NIFA and IFA. The four different indicators of Arctic ice—area, extent, thickness and volume—are estimated using univariate bivariate and multivariate models. These models consider the joint zero restriction for obtaining and evaluating nearly ice-free Arctic years. The research additionally looked into the possibility of advancement by utilising carbon capture and storage (CCS) - a technique for trapping greenhouse gas emissions and keeping them out of the atmosphere- which might foresee a bright future and delay the Nearly Ice Free Artic (NIFA) years. The study concludes that since the first NIFA years are already anticipated to happen in a very short period, CCS will not have any opportunity to grow and demonstrate its effectiveness. As a result, there is unlikely to be a delay of more than three years. Yet, there could still be hope for the Arctic's future.

1 Introduction

The Arctic region has an essential role in regulating and managing the planet's climate. Albedo feedback amplification loop is the phenomenon, known as the cycle that occurs when darker open water, which absorbs sunlight, replaces more reflecting Arctic sea ice. This happens due to ice loss caused by climate change and thus, eventually contributes to future climate change. There has been a concerning decline in the amount, thickness, and volume of arctic sea ice during the last few decades, and predictions indicate that the area may become seasonally ice-free in the next decades (Dauginis & Brown, 2021). The global climate systems, biodiversity, and human populations are all significantly impacted by this sharp decline, especially the mid-latitude patterns of air circulation and precipitation (Sewall & Sloan, 2004). Consequently, this is one of the most obvious and concerning signs of climate change. Moreover, climate change has major worldwide economic implications, therefore the significance of this research goes beyond its effects on the environment (Stern, 2008). Furthermore, a framework for assessing the economic impacts of Arctic ice loss is necessary for understanding the broader effects of climate dynamics in this area (Alvarez, 2020).

Understanding the dynamics of Arctic melting is essential for predicting future climate scenarios and developing strategies to mitigate the adverse effects of $CO2$ emissions from major industrial sources on both the environment and economies. While renewable energy and materials efficiency could make a significant contribution to industrial emission reductions, their joint potential is not enough to fully decarbonise the industrial sector. To reach net zero emissions, (International Renewable Energy Agency (IRENA), 2024) supports countries to define strategies where carbon capture and storage (CCS), carbon capture and utilisation (CCU) and carbon dioxide removal (CDR) may play a role. CCS is broadly recognised as having the potential to deliver low carbon heat and power, decarbonising industry and, more recently, its ability to facilitate the net removal of $CO2$ from the atmosphere (Bui et al., 2018). Therefore, this can be addressed as one promising solution for dealing with this crisis. CCS is a technology designed to capture carbon dioxide emissions from sources like power plants and manufacturing activities and store it underground to prevent it from entering the atmosphere (Bahman, Al-Khalifa, Al Baharna, Abdulmohsen & Khan, 2023). By preventing $CO2$ from entering the atmosphere, CCS can significantly contribute to achieving net-zero emissions targets (Johnsen, 2017). Therefore, this research will seek an answer to the question of whether or not this is possible to delay the arrival of the first NIFA years using CCS, and for how many years it is possible to delay the arrival of the mentioned crisis.

This research will provide the methodology and results of using point, interval, and density forecasts for four measures of Arctic sea ice coverage using area and extent, thickness, and volume to employ probabilistic assessment of the timing of the Nearly ice-free arctic years that adopted by (F. X. Diebold et al., 2022). Their research focused on projecting the timing of the first ice-free September, as September is referred to as the month with the least seasonal ice and exploring both an ice-free Arctic (IFA) and an effectively or nearly ice-free Arctic (NIFA) September. A notable aspect of their analysis is the enforcement of the joint constraint that these measures must simultaneously arrive at an ice-free Arctic where they sequentially considered pairwise blends of area with each of the other indicators. They have implemented their constrained

joint forecasting procedure in "carbon-trend" models that relate sea ice to atmospheric carbon dioxide ($CO2$) concentration with this time series denoted as $CO2C$ also in this research paper. Moreover, by employing linear carbon trends for both carbon-space and time-space they relate sea ice simply to time to project the future state of Arctic sea ice. This proposed study will enhance the previously utilised constraint bivariate and unconstrained univariate models by imposing the "all indicators should be vanishing together" constraint and using a multivariate constraint model. This approach aims to verify the consistency of their approaches and to make probabilistic forecasts of the arrival years of NIFA and IFA.

There are multiple conceivable contribution levels described earlier in various literatures. According to (Kocs, 2017), CCS can cut emissions from multiple sources, including stationary sources like power plants and industries, accounting for 60% (15 billion tonnes) of total CO2 emissions annually. The International Energy Agency (IEA) Blue Map (Radcliffe, 2010) scenario envisions a 19% contribution from CCS to global $CO2$ reductions by 2050, which would require capturing, transporting, and storing over 8 gigatonnes (Gt) of $CO2$ annually by 2050. This scenario also outlines a pathway to stabilise atmospheric CO2 concentrations at 450 parts per million (ppm) by 2050. This concluded based on the present rate of 0.04 gigatonnes per annum (Gtpa), it is estimated that to achieve net-zero by 2050, about 6 Gtpa of $CO2$ must be caught and stored by 2040, and over 8 Gtpa by 2050.

Therefore, this research will assess the carbon-trend results when carbon is measured as cumulative $CO2$ emissions ($CO2E$) as done in (F. X. Diebold et al., 2022). This will follow a further assessment based on the adjusted emission scenarios which will use a framework that has been suggested by IEA (Radcliffe, 2010). These will further be used to make probabilistic forecasts of the arrival years of NIFA and IFA which will proceed the way of the research through an answer.

The structure of the paper will be as follows: Section 2 earlier works of literature that provide knowledge and insight to this study, Section 3 presents the variables and data used in the study. Section 4 methodology of the methods that are used for estimation predictions and probabilistic analysis. Section 5 discussion and illustration of the results that this research has arrived at. Section 6 conclusion, which includes the study's primary conclusions, limitations, and recommendations for further research.

2 Literature

Previously in this field, climate models have made significant contributions to the understanding of the global and Arctic climates by capturing several drivers at high temporal and geographic precision. Thus, climate models were most likely to be taken into consideration for use in Arctic study. (Shen, Duan, Li & Li, 2021) assessed the capabilities of CMIP5 and CMIP6 models in simulating Arctic sea ice cover, finding that while CMIP6 models have reduced some biases seen in CMIP5, significant discrepancies remain, particularly during the summer months. Although these models have been highly valuable in understanding how the climate varies, they have shown limitations in terms of accurately predicting the loss of Arctic sea ice and frequently underestimating the magnitude of the recent reduction (Stroeve et al., 2012)and (Rosenblum & Eisenman, 2017). (F. Diebold & Rudebusch, 2022b) suggests that highly simplified dynamic

time series models can provide the same or even outperform the statistical projections of structural models. Such approaches are particularly useful for forecasting select climate outcomes because fundamental details of climate dynamics are not well understood, as evidenced by the diverse projections from various CMIP6 climate models (Notz & SIMIP, 2020). In particular, smaller-scale econometric and statistical models have proven useful for forecasting Arctic sea ice (Lei, Yuan, Ting & Li, 2016) and (F. Diebold & Rudebusch, 2022b) demonstrated how well they can estimate summer Arctic sea ice concentration. A collection of research involving modelling the Arctic decrease using sea ice thickness and volume (Stroeve & Notz, 2018) as well as sea-ice coverage (Stroeve et al., 2012). Consequently, in-depth evaluation and analyses of the modelling and measuring methodologies will be entailed. This study will evaluate the models by applying the methodology used in (F. X. Diebold et al., 2022) and additionally, it also combines multivariate modelling of the indicators with the all-in-one vanishing constraint. Combining multiple indicators of a latent variable can lead to better estimates by reducing the impact of measurement errors in each indicator (Joreskog, 1970) and (Goldberger, 1972). Consequently, by combining all of the individual indicators into a multivariate model, a better assessment and understanding of the dynamics of the sea ice can be obtained, given that the indicators have different measurement errors.

Carbon capture and storage (CCS) is broadly recognised as having the potential to play a key role in meeting climate change targets, delivering low carbon heat and power, decarbonising industry and, more recently, its ability to facilitate the net removal of CO2 from the atmosphere (Bui et al., 2018). Furthermore, utilising Life Cycle Assessments (LCA), several studies have investigated the environmental impacts of Carbon Capture and Storage (CCS) technologies. A complex weighting approach for LCAs was created by (Johnsen, 2017), particularly for amine-based post-combustion CCS in the Arctic. This approach provides an extensive framework for assessing the environmental trade-offs of CCS technology by examining the consequences of climate change, toxicity, and resource depletion, among other environmental categories. Building on this framework, (Bahman et al., 2023) offered an in-depth analysis of CCS technology used in various sectors. According to their research, CCS can significantly decrease CO2 emissions, helping the world reach its 2050 net-zero emission goals. Through the demonstration of case scenarios, they have highlighted the importance of CCS in mitigating the effects of climate change and highlight its useful applications. The implementation of CCS in the high Arctic presents both opportunities and constraints (Lubrano Lavadera et al., 2018). The paper drew attention to the distinct environmental circumstances found in the Arctic, which need specialised strategies for ensuring the effective implementation and monitoring of CCS technologies.

Probability assessments of the timing of an ice-free Arctic, an outcome with vital economic and climate consequences (Jahn, Randall, Holland & Senior, 2016). While earlier studies primarily used LCA approaches, this study report provides a statistical and probabilistic evaluation method to analyse the influence of CCS on postponing an ice-free Arctic. Through the integration of Shared Socioeconomic Pathways (SSP) scenarios and CO2 concentration levels, this probabilistic evaluation technique offers a more thorough and dynamic evaluation of the possible effects of CCS in the Arctic. This methodology provides an in-depth assessment of the environmental implications of CCS implementations in the Arctic region by evaluating the probabilities

and uncertainties related to such implementations. This gives an enhanced understanding of how CCS technology could be able to mitigate the effects of climate change in the Arctic. This is also essential for understanding the long-term effectiveness of CCS as a climate mitigation strategy and its role in preserving the unique and delicate Arctic ecosystem.

3 Data

This study will evaluate the four main measurements of Arctic sea ice: extent, area, volume, and thickness. The seasonal minimum of these indicators—that is, the monthly average for September—is the focus of our investigation. A detailed explanation regarding to calculation of the satellite observations can be obtained from (F. X. Diebold et al., 2022).

The whole procedure for data gathering and adjustment process for the required data set follows the approach used in the (F. X. Diebold et al., 2022). The National Snow and Ice Data Center's Sea Ice Index monthly dataset, Version 3, Dataset ID G02135, is the source of the data utilised for both Area and Extend. Initially, the pole hole was filled by applying an area adjustment of 1.19×106km2 to the SIA from the sample start to July 1987, $0.31 \times$ 106km2 from September 1987 to December 2007, and 0.029×106 km2 from January 2008 to the present, adopting the guidelines of (F. X. Diebold et al., 2022). The thickness data, which comes from PIOMAS at the Polar Science Centre and is published every day, has been converted into monthly averages. PIOMAS also provides sea ice volume data; it estimates the total volume of sea ice by combining surface coverage and thickness data. In particular, as $Thickness \times Area$. Several sea-ice indicators, including sea-ice area (SIA), sea-ice extent (SIE), sea-ice thickness (SIT), and sea-ice volume (SIV), are used in this study. Annual data from September encompassing the years 1979 to 2021 are used. Beginning in 1979, data preprocessing creates a new index that represents the year. It is noteworthy to emphasise that the $CO2$ emission and CCS portions of the study will make use of the measurements from 1979 to 2023. Future years will be left for prediction and adjustment. Additionally, making sure the variables of interest have no missing values is essential.

3.1 CO2 Concantration

The NOAA Global Monitoring Laboratory 20 provides historical $CO2$ atmospheric concentration data (in parts per million, PPM) for the years 1979 to 2021. $CO2$ is measured at Mauna Loa Observatory, Hawaii. Values from the SSP Public Database (Version 2.0) are used for the Shared Socioeconomic Pathways (SSP) Scenario for the years 2022-2100. Each scenario is derived from the IAM Scenarios spreadsheet following (F. X. Diebold et al., 2022). Between 2005 and 2100, there are eleven data points in each of the three scenarios. For the years 2022-2100, missing data points were filled with linear interpolation. As a direct indicator of the quantity of heat-trapping gases in the atmosphere, which plays a major role in the melting of Arctic ice, the atmospheric $CO2$ concentration ($CO2C$) is provided. Direct air sampling is used to measure this concentration, and there is very little measurement error. Through the consideration of many potential socioeconomic changes and accompanying greenhouse gas emissions, the SSP scenarios provide a comprehensive framework for assessing future climate change implications.

This can be observed from the Figure 1.

3.2 CO2 Concentration under different SSPs

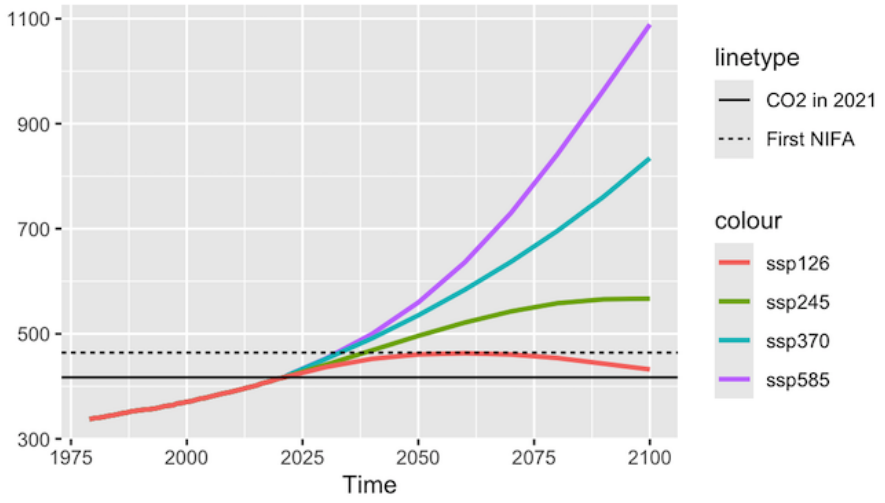

Figure 1: Atmospheric CO2 Concentration Scenarios for Carbon Capture and Storage

3.3 CO2 Emission

The study replicated in this paper uses cumulative $CO2$ emissions data from (Rogelj et al., 2021), with processing carried out according to previous procedures (F. X. Diebold et al., 2022). While, emissions from changes in land use are based on estimates of deforestation, $CO2$ emissions are computed indirectly from statistics on energy, fuel usage, and cement manufacturing.

The Carbon Capture and Storage Scenario from the IAM Scenarios spreadsheet is incorporated using values from the SSP Public Database (Version 2.0) for the years 2022-2100, just as it was done previously. Data was only available for SSP2 4.5 and SSP1 2.6 so this procedure only followed for them. Eleven data points covering the years 2005 to 2100 were supplied, with yearly measurements in megatonnes (Mt/year). As a result, the data points were converted to gigatonnes on an annual basis. Data was zero before 2030 when it was utilised as a starting point in 2030. For the missing data points from 2030 to 2100 to apply to our cumulative emission in our data set, they were filled in using linear interpolation to create a cumulative version of the data.

In the direction of the International Energy Agency's (IEA) Blue Map scenario (Radcliffe, 2010), the SSP5 8.5 and SSP3 7.0 scenarios were developed. With a specific target of 6 gigatonnes per annum (Gtpa) of $CO2$ to be caught and stored by 2040, the current amount is set at 0.04 Gtpa. 8 Gtpa by 2050, with further increases predicted up to the year 2100 based on the supposition that technology will advance and allow for greater capture, with the pace of progress fluctuating with time. 10 Gbps by 2060, 16 Gbps by 2070, 20 Gbps by 2080, 25 Gbps by 2090, and 30 Gbps by 2100 are the next targets. Once again, those data points were interpolated, created a cumulative format,

Figure 2 illustrates scenarios for $CO2$ emissions and scenarios with changes for CCS:

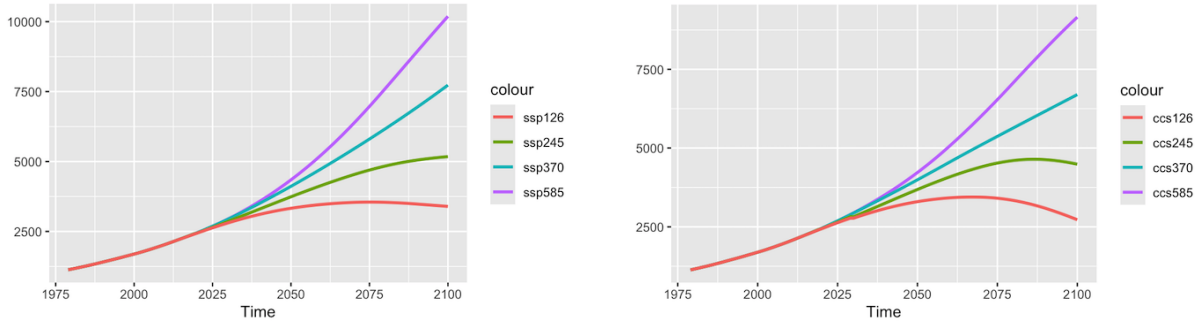

(a) CO2 Emission Scenarios

(b) CO2 Emission Scenarios for CCS

Figure 2: Comparison of CO2 Emission Scenarios

Findings from (Blackford, 2022) indicate that only massive, catastrophic leaks would seriously harm the ecosystem. Furthermore, to guarantee the safety of CO2 storage operations, comprehensive risk assessment frameworks that combine modelling and experimental methods are necessary (Gholami, Raza & Iglauer, 2021). This indicates that there is a low chance of a leak, making it unimportant to take into account in this study.

4 Methodology

The models and methods used to evaluate the specific relation between four Arctic sea indicators and atmospheric CO2 concentration using the linear carbon trend, as previously described in the work (F. X. Diebold et al., 2022), are described in this section.

4.1 Carbon-Trend Model

Numerous studies, including (Johannessen, 2017), have already established a linear empirical link between $CO2$ and the observed Arctic sea-ice area.

The identical linear carbon-trend relationship will be used in this study to assess the linear empirical relationships between observed arctic sea-ice indices, including coverage (measured by area and extent), volume, and thickness. This linear carbon-trend relationship is fitted by the observed data, which may be expressed as follows:

$$\mathrm{x}_t = \alpha + \beta \mathrm{CO2}_t + \epsilon_t \tag{1}$$

x_t represents the four indicators: area, extent, thickness, and volume. $\mathrm{CO2C}_t$ represents the atmospheric $CO2$ concentration, and ϵ_t indicates deviations from the linear fit. The regression intercept, α, is used to calibrate the sea-ice coverage, whereas the slope, β, measures the Arctic carbon reaction. A negative value for β represents the shrinking covering of Arctic sea ice as greenhouse gases accumulate in the atmosphere.

This work computes linear carbon trends in the Time-Space and Ice-Carbon Spaces. According to the Carbon-Space model, SIA will only decrease proportionately in response to increases in $CO2C$; rather, it will respond linearly to $CO2C$. The predicted trends of $CO2C$ concentrations over time are followed by non-linear curvatures in the SSP scenarios. Consequently, the

estimated sea-ice time trend will be decreasing at an increasing rate due to a growing rate of increase in the concentration of $CO2$ over time. To address the non-linear temporal trend issue, this study uses the same fitted linear relationship as sea ice indicators to $CO2$ concentration to pass the non-linear concentration schedule given by the SSP scenarios. The positive aspect of this is that it converts linear elements in ice-carbon space into nonlinear elements in ice-time space.

4.1.1 Unconstrained Univariate Model

We consider four related sea ice measures in this model: sea ice volume (SIV_t) at time t, sea ice area (SIA_t), sea ice thickness (SIT_t), and sea ice extent (SIE_t). Every one of these measurements is expressed as a function of the CO_2 concentration $CO2C_t$; the error term is ϵ_t, the intercept is α, and the coefficient for the CO_2 concentration is β.

$$\begin{aligned} SIA_t &= \alpha_a + \beta_a \cdot CO2C_t + \epsilon_t \\ SIE_t &= \alpha_e + \beta_e \cdot CO2C_t + \tau_t \\ SIT_t &= \alpha_t + \beta_t \cdot CO2C_t + \kappa_t \\ SIV_t &= \alpha_v + \beta_v \cdot CO2C_t + \upsilon_t \end{aligned} \tag{2}$$

Seemingly Unrelated Regression (SUR) is the method used because these metrics are likely to be interrelated. To produce more accurate and efficient parameter estimations, the SUR model takes into consideration any possible correlations between the error terms ($epsilon_t$) of the various equations (Beasley, 2008). (See the estimation method section for a thorough description of the estimation method and technique.)

This structure allows the estimation of each linear regression individually using the ordinary least squares (OLS) approach because all equations share the same regressor ($C0_2$ concentration). By doing this, the SUR framework is used to account for the interdependencies between each sea ice measure and the CO_2 concentration, essentially capturing the linear relationship between each of them. The impact of CO_2 concentration on several aspects of sea ice dynamics is better-understood thanks to this thorough modelling technique.

4.1.2 Constrainted Bivariate Models

Using a combined modelling approach in the bivariate models ensures that zero sea-ice measures are taken simultaneously by modelling two or more sea-ice indicators concurrently. For instance, the bivariate linear carbon trend model is given by:

$$\begin{aligned} x_t &= \alpha^x + \beta^x \cdot CO2C_t + \epsilon_t^x \\ y_t &= \alpha^y + \left(\frac{\alpha^y \beta^x}{\alpha^x}\right) \cdot CO2C_t + \epsilon_t^y \end{aligned} \tag{3}$$

Here, depending on the scenario being assessed, y_t can represent extension, thickness, or volume, but x_r always illustrates the Area indication. The measures will all reach zero at the same time thanks to this combined restriction. The linear regression regressors are no longer the same in this joint model. To produce more accurate and efficient parameter estimates, the

Seemingly Unrelated Regression (SUR) estimation process takes into consideration any possible correlations between the error components of the various equations. This method helps in understanding the interdependent effects of $CO2$ concentration on two sea ice indicators at once.

4.1.3 Multivariate Constraint Model

$$\begin{aligned} x_t &= \alpha^x + \beta^x \cdot CO2C_t + \epsilon_t^x \\ y_t &= \alpha^y + \left(\frac{\alpha^y \beta^x}{\alpha^x}\right) \cdot CO2C_t + \epsilon_t^y \\ z_t &= \alpha^z + \left(\frac{\alpha^z \beta^x}{\alpha^x}\right) \cdot CO2C_t + \epsilon_t^z \\ w_t &= \alpha^w + \left(\frac{\alpha^w \beta^x}{\alpha^x}\right) \cdot CO2C_t + \epsilon_t^w \end{aligned} \tag{4}$$

The Area, Extent, Thickness, and Volume indicators are represented by the symbols x_t, y_t, z_t, and w_t, in this case. The simultaneous zeroing of all measures is guaranteed by this joint constraint. Each indicator's error terms are ϵ_t^i (where i can be area, extension, thickness, or volume). Due to the same reasoning as bivariate constraint models, it uses the same estimation process as SUR regression (see the next subsection for a thorough explanation).

4.1.4 Estimation Method

Our primary concern is efficiency in estimation and accounting for correlated error terms in separate equations. Therefore, the Seemingly Unrelated Regression (SUR) model is suitable for our analysis. The SUR model offers several advantages. The Seemingly Unrelated Regression (SUR) model provides significant efficiency gains when error terms across different equations are correlated. This is particularly useful because it leads to more accurate estimates than independent estimation of each equation. Additionally, the SUR model allows for the estimation of separate regression equations for each dependent variable, offering flexibility and improved model fit. By accounting for correlated errors, the SUR model enhances the precision of estimated coefficients, which is crucial for studies involving common influencing factors, such as CO_2 concentration affecting sea ice indicators (Saraceno, Alqallaf & Agostinelli, 2021).

In this paper, we replicate the estimation process using the SUR model to account for the potential correlations between the error terms of different sea ice indicators. By using the SUR model, we aim to obtain more efficient estimates compared to estimating each equation separately. For the univariate case, estimation can be carried out separately for each indicator using Ordinary Least Squares (OLS) regressions since they all have the same regressor. However, given that the SUR model involves potentially heteroskedastic and correlated errors across equations, we use the Feasible Generalized Least Squares (FGLS) estimation method. This approach allows for consistent and efficient estimation of the model parameters, taking into account the correlation structure of the residuals. The estimation process using the SUR model involves several key steps. First, it is essential to handle constraints by ensuring that the sea ice measures simultaneously reach zero, thereby imposing a joint constraint on the model. Next, the specified model is used to predict the values of the dependent variables. Following prediction, the residuals

(errors) for each equation are calculated. These residuals are then used to construct the error matrix.

To estimate the covariance matrix Ω of the error terms, we apply m regressions, one per unit, to estimate β_j by OLS, where $j = 1, \cdots, m$. Let e_i be the $n \times 1$ vector of OLS residuals for unit i; then the (co)variances σ_{ij} are estimated by $s_{ij} = \frac{1}{n}\sum_{t=1}^{n} e_{it}e_{jt}$. The $mn \times mn$ matrix $\hat{\Omega}$ is estimated by replacing σ_{ij} in Ω by s_{ij}.

The FGLS estimator, b_{FGLS}, is computed by substituting the estimated covariance matrix $\hat{\Omega}$ into the GLS estimator formula:

$$b_{\text{FGLS}} = (X^T\hat{\Omega}^{-1}X)^{-1}X^T\hat{\Omega}^{-1}y$$

where X is the matrix of regressors, and y is the vector of dependent variables.

In R, the FGLS estimation for the SUR model can be performed using the `nlsystemfit()` function with the method specified as "SUR". The function `nlsystemfit(method = "SUR")` handles the estimation, incorporating the described steps of the FGLS method.

4.2 Probabilistic assessment of Sea-Ice Disappearance

To assess the variability and uncertainty in the predictions. Employment of bootstrap simulations method involves repeatedly resampling the data with replacement, refitting the models to each bootstrap sample, and generating a distribution of possible future scenarios. The steps in the bootstrap method include generating a bootstrap sample by random sampling with replacement from the original dataset, fitting the probabilistic model to the bootstrap sample, predicting future values using the refitted model, and repeating these steps a large number of times (e.g., 1000 iterations) to build a distribution of predictions. The results from the bootstrap simulations are analyzed to calculate the probabilistic distribution of Nearly Ice-Free Arctic (NIFA) years. This involves applying a function to each bootstrap sample to identify the year when the Arctic becomes ice-free (i.e., ice thickness or extent drops to zero) and summarizing the distribution of predicted NIFA years to derive key statistics such as mean, standard deviation, median, and confidence intervals. Finally, the results from the probabilistic model and bootstrap simulations are combined to provide a detailed analysis, comparing the predicted NIFA years under different scenarios, such as with and without CCS interventions. This methodology provides a robust framework for predicting Arctic ice dynamics in response to $CO2$ concentration changes and management interventions, balancing simplicity and complexity to ensure both interpretability and accuracy in the predictions.

5 Results

This section will provide the results for the carbon concentration, carbon emission, and emission scenario for the incorporation of CCS. R-version 4.3.3 is used to conduct the results in the tables and figures.

Figure 3: Univariate and Bivariate Models in CO2 Concentration For Carbon-Space Under SSP3.70

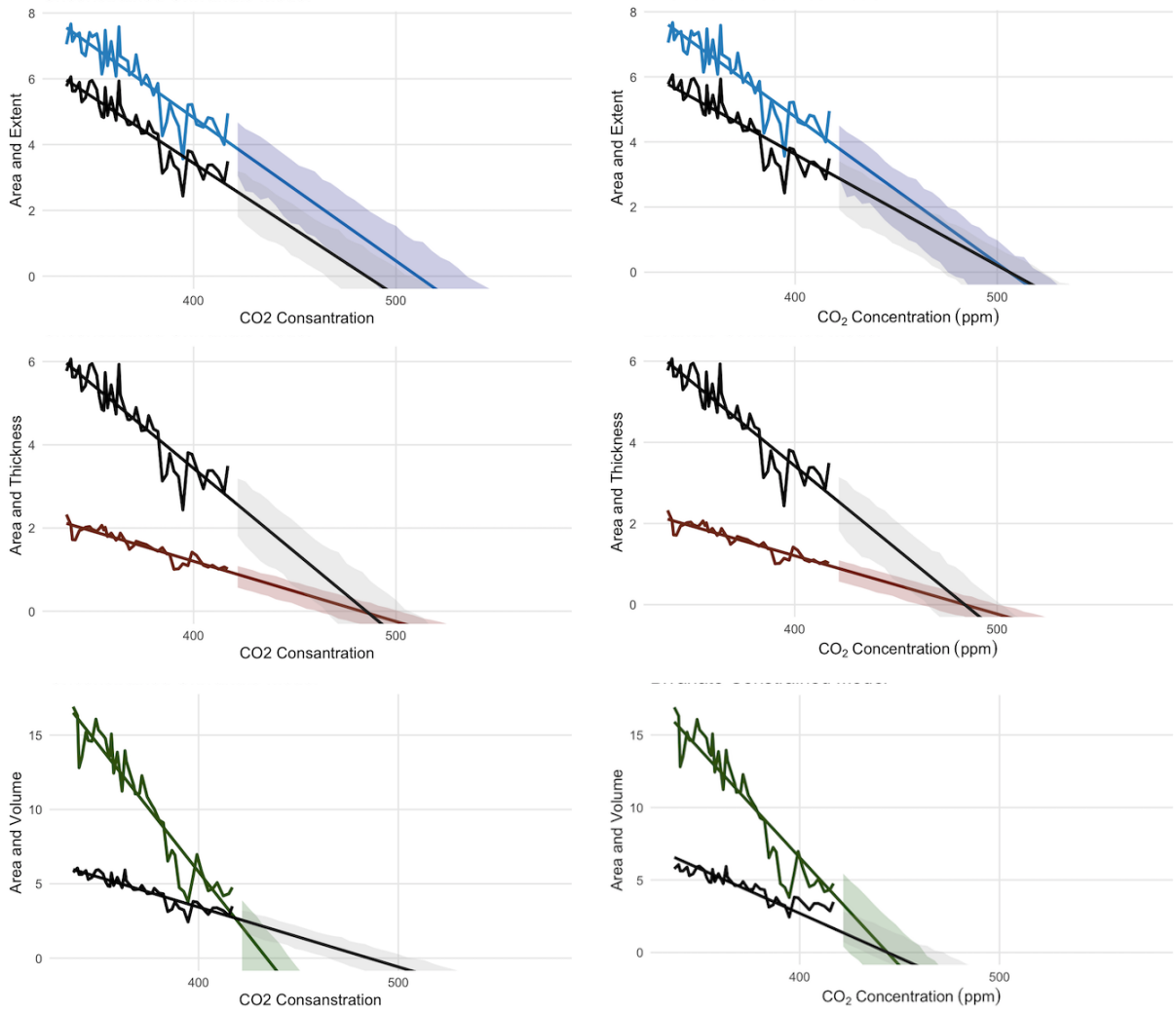

Observation and fitted line estimates for several models utilising regression techniques that were previously described for each model in the Figure 3 section of Methodology. SIA, SIE, SIT, and SIV are denoted by the colours black, blue, red, and green, respectively. Regular downward-sloping lines were fitted to the sample data to represent linear carbon trends, while irregular lines were used to observe the indicators. Two sea-ice measurements are shown against the atmospheric $CO2$ concentration ($CO2C$) in each graph.

As desired replication findings, Figure 3 displays estimates of the linear carbon trend for SIA, SIE, SIT, and SIV (displayed on the left side) as well as the bivariate combinations (displayed on the right side) from 1979 to 2021. The figure is illustrated by the earlier findings by (F. X. Diebold et al., 2022). As anticipated, there has been a downward trend in both the thickness and coverage of Arctic sea ice, although there has been a greater trend in volume throughout the sample. The 90% interval projections based on simulation and 1000 bootstraps produced results that were somewhat predicted. Certain intervals are always broader than others because the models are restricted in the expectation domain not in their shock variances.

Additionally, it was noted that using 10 seeds for the bootstrap algorithm (refer to Appendix

seeds produced a far less diverse upper-lower bound for observation, making the confidence interval visuals appear smoother and more in line with the findings of (F. X. Diebold et al., 2022). Moreover, using the (inverse) concentration schedule SSP3 7.0 of Figure 1 and the fitted carbon trends of Figure 3, the implied time trends are derived. As a result, a time in ice-time space corresponds to every concentration in ice-carbon space. (See Appendix for figures.)

Figure 4: Multivariate Model For CO2 Concentration in Carbon-Space under SSP3 7.0

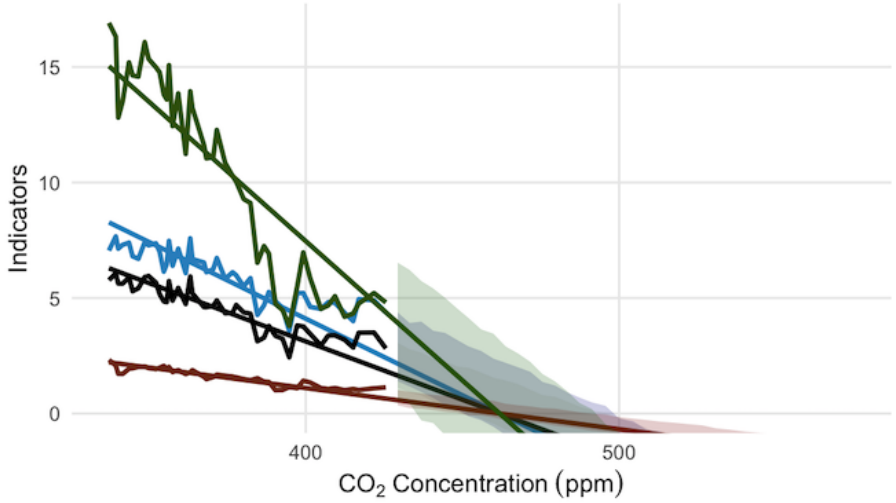

All indicators reaching IFA constraint for the multivariate model with all sea indicators (*Multi*) from 1970–2023 are shown in Figure 4. In simulation-based 90% interval forecasts, the unstable widening of the intervals was once again observed using 1000 bootstrap. The combined model for the right side of the graphs in Figure 3 is displayed in Figure as the combined representation of the bivariate models of each indicator combination of other indicators with SIA.

The Table 1 contained a summary of the qualitative observations and interpretations of the models in Figure3 and Figure 4. The projected b values and all $R2$ values yield two d.p. and the same significant value. The bivariate constrained estimated first-IFA concentrations are 509 ppm, 488 ppm, and 445 ppm when SIA is modelled in combination with SIE, SIT, and SIV. This demonstrates alignment with earlier results (F. X. Diebold et al., 2022). Moreover, it is worthwhile to mention that the SIA is computed using the definition of being below 1 km found in the current literature including (Stroeve & Notz, 2018). Nevertheless, no similar definitions of practically ice-free concentrations for SIT and SIV exist in the literature, therefore we only address the first NIFA in SIA.

Table 1: September Arctic Sea-Ice Indicators: Linear CO_2 Carbon Trend Estimates and Projections (Under SSP3 7.0)

			First IFA		First NIFA (Area)	
Model	$\hat{b}$	R^2	CO2C (ppm)	year	CO2C (ppm)	year
Unconstrained Univariate Models						
SIA	−0.04	0.84	488	2039	464	2033
	(0.003)					
SIE	−0.04	0.80	514	2045		
	(0.003)					
SIT	−0.01	0.86	484	2038		
	(0.001)					
SIV	−0.17	0.90	437	2026		
	(0.009)					
Constrained Bivariate Models						
SIA+SIE	−0.03	0.82	509	2044	480	2037
	(0.003)					
SIA+SIT	−0.04	0.84	487	2039	460	2032
	(0.002)					
SIA+SIV	−0.06	0.58	444	2028	430	2024
	(0.003)					
Constrained Multivariate Model						
Multi	−0.05	0.73	464	2033	444	2028
	(0.003)					

Among all indicators only the SIV indicator blended with SIA is greater than the first NIFA carbon levels in the multivariate model. Additionally, the multivariate model shows lower levels of carbon concentration for both the first IFA and the NIFA when compared to the baseline bivariate model of SIE with SIA. This corresponds to earlier NIFA and IFA years estimated using a multivariate model.

The range of the anticipated first-IFA concentrations is reduced by the bivariate constrained blending of SIA with the other indicators (F. X. Diebold et al., 2022); hence, a multivariate model will also be applied to the same circumstance. The limited bivariate range is 509 ppm - 444 ppm = 65 ppm, while the univariate IFA range is established as 514 ppm - 437 ppm = 77 ppm. Using a multivariate model, the remaining carbon budget for the IFA year is 464 ppm - 426 ppm = 38 ppm, given that the carbon concentration level in 2023 is 426 ppm.

Additionally, the remaining carbon budget for the NIFA year is estimated to be 444 ppm - 426 ppm = 18 ppm, which is significantly less than the budget determined by the paper (F. X. Diebold et al., 2022) using the univariate SIA model. Whereas, it is noticeable that the multivariate model's IFA concentration level matches the NIFA year of the SIA univariate model.

Figure 5: Univariate and Bivariate Models For CO2 Emission in Carbon-Space a Under SSP3.70

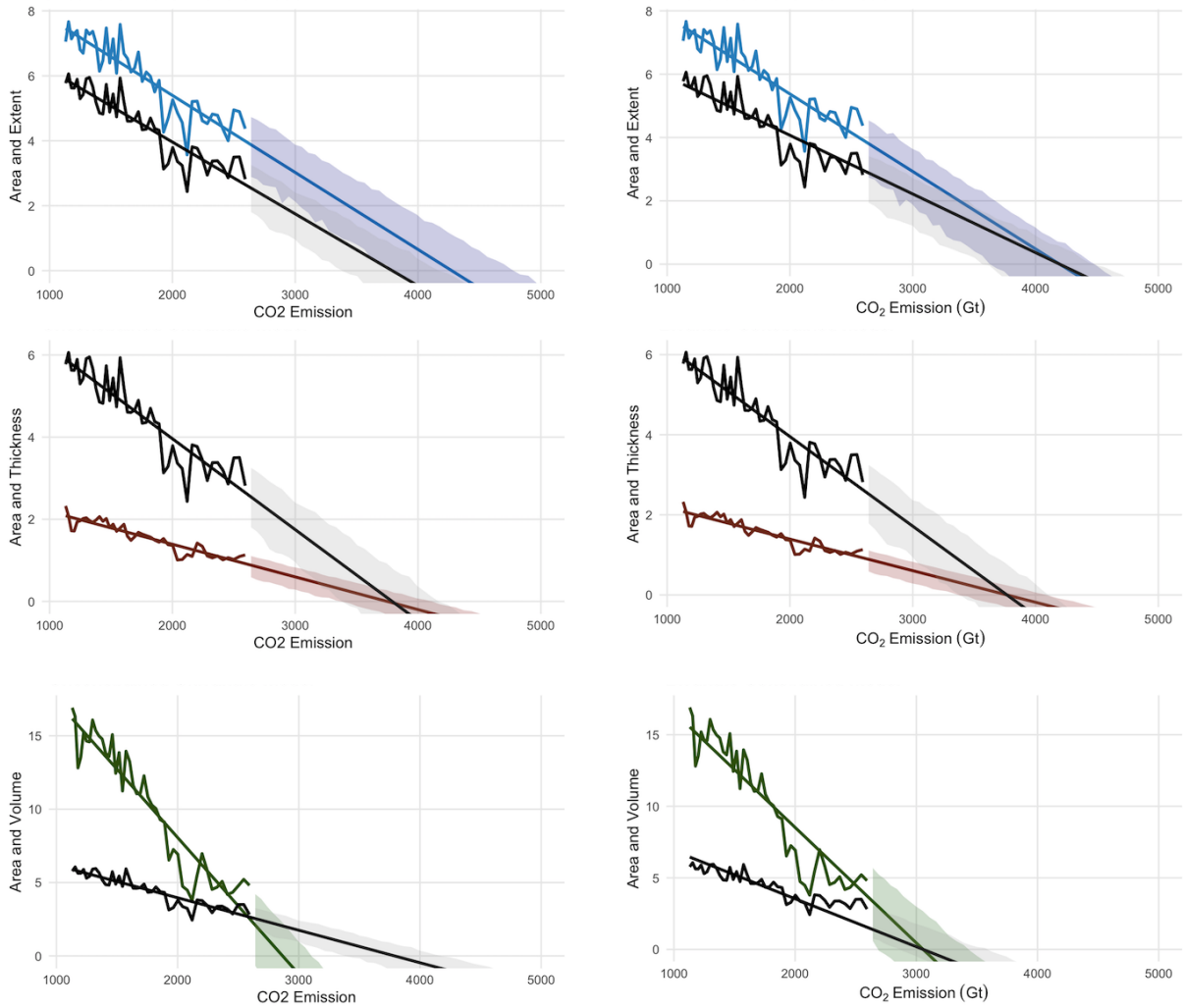

*CO*2 emission under CCS interventions is shown in Figure 6, and the *CO*2 emissions-based carbon-trend results are shown in Figure 5.(To view the implied carbon trends in ice-time space, see Appendix.) The emission estimates correspond quite well with the previous conclusions based on the concentration, which is to be expected given that the *CO*2 concentration and emission are not expected to display distinct patterns. As a result, the emissions' linear carbon trend seems to fit each measure of Arctic sea ice well. Figure 10 (see Appendix) has the same conclusions that apply to the multivariate model account for *CO*2 emission numbers as well as for CCS for carbon and time-space.

Figure 6: Univariate and Bivariate Models For CO2 Emission CCS Scenarios in Carbon-Space a Under SSP3.70

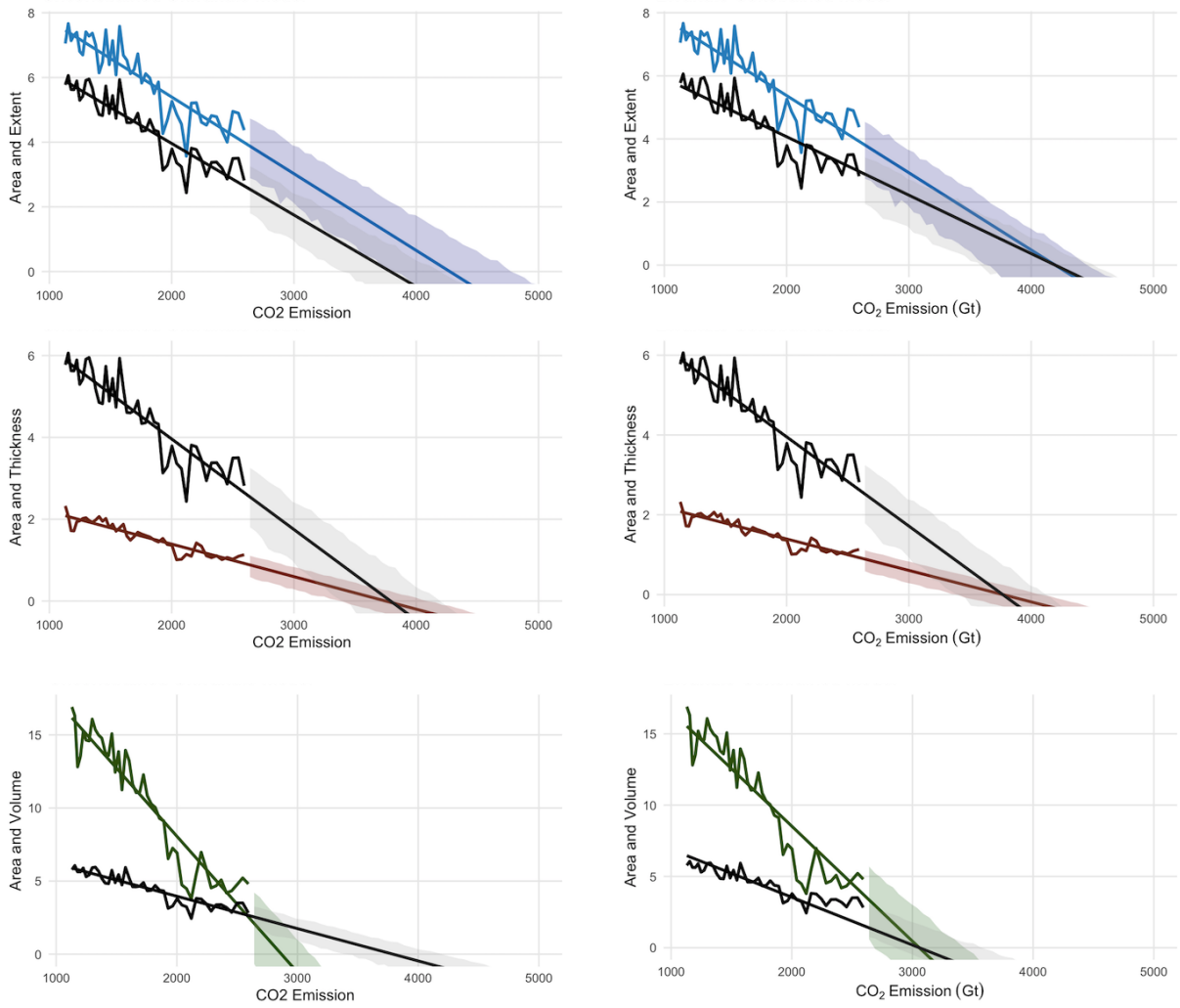

There is an overall increase in the NIFA and IFA years Table1 when carbon capture and storage scenarios are used. In addition, projections and estimations of sea-ice indicators such as $CO2$ emissions without the use of CCS Table 5 (see Appendix) shows slightly different from the previous study was expected as this study used observations up to 2023 instead of 2021. Main findings include the corresponding $CO2E$ for the first NIFA (univariate SIA) of 3350 Gt, which, when compared to the current cumulative emissions of approximately 2593 Gt under SSP3 7.0, indicates that only two years will remain before the carbon budget drops to approximately 757 gt. Previously, it obtained 776 gt by taking the present year 2021 as the point at which the Arctic Ocean will almost entirely be free of ice.

Additionally, in the first NIFA years, bivariate and multivariate models indicate a 10-year delay for SIE when combined with the SIA model, a 6-year delay for SIT with the SIA and multivariate model, and only a 3-year delay for SIV with the SIA model. Delays in the first IFA years in constrained bivariate and multivariate models are generally greater compared to those in the first NIFA years. This is not as strange as first thought because, according to the International Energy Agency's (IEA) Blue Map Scenario, over 8 Gtpa of carbon dioxide

could be captured by 2050. This amount has the potential to drastically affect the level of CO2 concentration. In contrast, the SSP3 7.0 scenario's emission levels will be high enough to experience the first NIFA years even before 2050. The fact that 0.04 Gtpa to 6 Gtpa are still effective even under SSP3 7.0 suggests that while the delay may not be sufficiently significant to cause the NIFA years to be greatly delayed, it is still noticeable.

Table 2: September Arctic Sea-Ice Indicators: Linear CO2 Carbon Trend Estimates and Projections for utilisation of CCS as CO2 Emission (Under SSP3 7.0)

			First IFA		First NIFA (Area)	
Model	$\hat{b}$	R^2	CO2C (ppm)	year	CO2C (ppm)	year
Unconstrained Univariate Models						
Area	−0.0022	0.83	3829	2047	3350	2038
	(0.00015)					
Extent	−0.0024	0.79	4326	2056	NA	NA
	(0.00018)					
Thickness	−0.0008	0.85	3775	2046	NA	NA
	(0.00005)					
Volume	−0.0093	0.90	2888	2029	NA	NA
	(0.00048)					
Constrained Bivariate Models						
SIE+SIA	−0.0019	0.81	4214	2054	3667	2044
	(0.00014)					
SIT+SIA	−0.0022	0.83	3774	2046	3349	2038
	(0.00012)					
SIV+SIA	−0.0034	0.59	3091	2033	2787	2027
	(0.00018)					
Constrained Multivariate Model						
Multivariate	−0.0030	0.73	3222	2046	2906	2034
	(0.00015)					

5.1 Probabilistic Assessment of Sea-Ice Disappearance and Comparison with the CCS scenarios

Assessing the approximations to their whole probability distributions is the aim of this section. In contrast to our previous first NIFA point projections, the random variation is also considered here. As a result, in addition to evaluating the mean, median, and mode of the first-NIFA distributions, other moments and associated statistics (such as standard deviation, skewness, kurtosis, and the percentiles for the left and right tails) may additionally be evaluated.

Table 3: September Arctic Sea-Ice Indicators: Probability Distributions of *SIA* First September NIFA Years

	Mean	**Median**	**Mode**	**SD**	**Skew**	**Kurt**	**5%**	**20%**	**80%**	**90%**
SSP5 8.5										
SIE+SIA	2031	2031	2031	3.29	-0.33	2.79	2025	2028	2034	2036
SIT+SIA	2030	2031	2031	2.30	-0.56	3.15	2026	2029	2032	2034
SIV+SIA	2024	2024	2023	1.55	0.68	2.97	2022	2023	2025	2027
Multi	2028	2028	2028	1.99	0.37	2.78	2025	2026	2030	2031
SSP3 7.0										
SIE+SIA	2033	2033	2034	3.15	-0.31	2.97	2027	2030	2036	2038
SIT+SIA	2031	2031	2032	2.41	-0.48	3.12	2026	2029	2033	2034
SIV+SIA	2024	2024	2023	1.57	0.65	2.88	2022	2023	2025	2027
Multi	2028	2028	2028	2.05	0.39	2.83	2025	2026	2030	2032
SSP2 4.5										
SIE+SIA	2037	2037	2036	4.36	-0.28	2.73	2029	2033	2041	2044
SIT+SIA	2034	2035	2034	3.25	-0.38	3.15	2028	2032	2037	2039
SIV+SIA	2025	2025	2023	2.12	0.68	3.27	2022	2023	2027	2029
Multi	2030	2030	2029	2.64	0.31	2.72	2026	2028	2032	2035
SSP1 2.6										
SIE+SIA	2044	2043	2041	9.98	1.51	8.24	2030	2036	2050	2061
SIT+SIA	2039	2039	2038	5.78	0.30	3.26	2029	2034	2043	2048
SIV+SIA	2025	2025	2025	2.43	0.78	3.45	2022	2023	2027	2030
Multi	2032	2032	2029	3.50	0.44	2.79	2027	2029	2035	2038

The Table 3 indicates some discrepancies between your replication and the original study. Specifically, in every scenario, the pair of coverage SIE and SIA reveal somewhat unrelated findings, but most significantly in SSP1 2.6.

Considering the deterministic trend, these shocks might be viewed as random variables that introduce variability. The shocks often follow a probability distribution, like the normal distribution, and can be either positive or negative. However, the failure to acquire identical findings may be due to ignorance about the distribution. To effectively represent the random changes, more information, presumptions, and processing resources are needed when including stochastic shocks. Not having enough knowledge about the stochastic shocks inclusion methodology therefore might be the reason for the inconsistency in the results. The research was conducted using the bootstrapping approach, which involves resampling the residuals with replacement. The cause for the discrepancy may be due to the inclusion of seeds in the (F. X. Diebold et al., 2022) study, or not knowing about the resampling methodology with enough detail. The main finding, nevertheless, is that the 80% probability of having a nearly ice-free Arctic by 2033 is for model SIT with SIA consistently obtained, as well as the central tendencies of the distributions of NIFA years in Table 3 for all mean, mode, and median are generally being a bit earlier than the corresponding years in Table 1. Furthermore, in the best-case scenario with an 80% confidence

interval, the latest first NIFA was continuously attained by SIE with the SIA model.

According to the multivariate model, there is an 80% probability that the first NIFA will occur by 2030. This forecast agrees with the 80% mean of the first NIFA years. (which was determined by using the second column from the right's mean). Regarding the $CO2$ concentration results, they were, according to the Table 6(see Appendix), at least as consistent with earlier studies as the CO2 emission probability distribution during the first NIFA years of the SIA.

Table 4: September Arctic Sea-Ice Indicators: Probability Distributions of *SIA* First September NIFA Years

	Mean	**Median**	**Mode**	**SD**	**Skew**	**Kurt**	**5%**	**20%**	**80%**	**90%**
SSP5 8.5										
SIE+SIA	2037	2037	2039	3.96	-0.46	2.78	2029	2033	2040	2042
SIT+SIA	2034	2035	2036	3.22	-0.51	2.82	2028	2032	2037	2039
SIV+SIA	2027	2026	2026	1.95	0.61	2.96	2024	2025	2028	2030
Multi	2030	2030	2029	2.48	0.21	2.97	2026	2028	2032	2034
SSP3 7.0										
SIE+SIA	2037	2038	2038	4.37	-0.31	2.72	2029	2034	2041	2044
SIT+SIA	2035	2035	2036	3.42	-0.47	2.78	2028	2032	2038	2040
SIV+SIA	2027	2026	2026	1.97	0.63	2.94	2024	2025	2028	2030
Multi	2030	2030	2029	2.57	0.24	2.99	2026	2028	2032	2034
SSP2 4.5										
SIE+SIA	2041	2041	2045	4.98	-0.30	2.63	2032	2036	2045	2048
SIT+SIA	2037	2038	2039	4.11	-0.51	2.84	2029	2034	2041	2043
SIV+SIA	2027	2027	2026	2.36	0.75	3.36	2024	2025	2029	2032
Multi	2032	2032	2033	3.22	0.07	2.45	2027	2029	2034	2037
SSP1 2.6										
SIE+SIA	2046	2046	2047	8.94	1.24	8.13	2034	2038	2052	2061
SIT+SIA	2041	2041	2042	5.90	0.06	2.91	2031	2035	2046	2050
SIV+SIA	2028	2027	2026	2.65	0.85	3.67	2024	2025	2030	2033
Multi	2033	2033	2033	3.78	0.15	2.64	2027	2029	2036	2039

The panels of Figure 6 projections display the carbon-space depicted confidence intervals for integrating CCS, along with their quantitative insights and Table 2 illustrations. The appendix Figure 12 and Figure 13 have indicated projections for time-space and multivariate models under carbon and time-space, respectively. Results under the CCS situations shown in Table 4 are evaluated probabilistically.

NIFA by 2036 with a confidence level of less than 80% was noted. This only leads to a three-year delay. Furthermore, in 80% of SSP circumstances, the NIFA arrival delay is three years. Changing the 95% percentage does not take into consideration any further delays. Furthermore, the Mean Mode Median for all situations, both separately and collectively, demonstrates the 3-year delay once more, except for the 5-year mode increase in SSP2 4.5.

6 Conclusion

This study enhanced the analysis by applying and assessing the impact and potential delay that could result from the use of carbon capture and storage techniques. It also successfully replicated previous findings on the predictability of disappearing Arctic sea ice using joint zero-constraint carbon trends.

The findings indicate that, even in the case of carbon capture and storage scenarios, it is not possible to postpone the first NIFA years by a considerable amount. This is because, with the first NIFA predicted to occur in the mid-30s, CCS will not have had enough time to develop and capture significant amounts during that particular time frame. It is not possible to postpone the first NIFA for longer than three years, even when the emission level drops to zero with CCS. The highly optimistic "net zero by 2050" SSP1 2.6 scenario is still the only one that can delay significantly the occurrence of the first NIFA years. Governments are committed to preventing global average temperature increases to well below 2°C over pre-industrial levels, ideally below 1.5°C, as doing so would greatly reduce the risks and effects of climate change (IPCC 2018). To maintain it and stop NIFA from arriving for more than three years is not possible even with the CCS approach. However, CCS remains a viable strategy for maintaining the Arctic's full seasonal disappearance; alternatively, it can be employed to postpone the appearance of a new NIFA or to prevent the achievement of the initial IFA.

Nevertheless, the study's reliance on historical data and linear models may not fully capture every aspect of Arctic ice dynamics, and the inclusion of specific scenarios increases uncertainty. Undoubtedly, there are a lot of neglected components like climate feedback models, such as albedo Arctic sea-ice reduction, that could have an impact on how accurate our point and interval projections are. Some of these factors could accelerate or slow the melting of sea ice, but this research does not address them. These include tipping points related to methane release from permafrost melting (Chylek et al., 2022) that may encourage an even steeper decline in sea ice, and extreme internal variation that may cause a warming hiatus (Miller & Nam, 2020) that slows loss. Although the CCS scenarios are generated and employed by the theoretical framework, the research conducted in this paper does not encounter the uncertainty surrounding them. Global agreements, financial incentives, and regulatory changes all have a significant role in the deployment of these technologies; nevertheless, geopolitical and economic factors that may influence the acceptance and implementation of CCS are not taken into account in this study.

Future research should examine the long-term effects of CCS beyond the mid-30s, especially its capacity to preserve the seasonal retreat of Arctic ice and postpone the advent of successive NIFA years, to enhance our understanding of and efficacy of climate intervention strategies.

References

Alvarez, L. (2020). A framework for assessing the economic impacts of arctic change. *Arctic Economics*, *8*, 101-120. Retrieved from https://doi.org/10.1016/j.arceco.2020.101120 doi: 10.1016/j.arceco.2020.101120

Bahman, N., Al-Khalifa, M., Al Baharna, S., Abdulmohsen, Z. & Khan, E. (2023). Review of carbon capture and storage technologies in selected industries: potentials and challenges. *Reviews in Environmental Science and Bio/Technology*, *22*, 451–470. Retrieved from https://doi.org/10.1007/s11157-023-09649-0 doi: 10.1007/s11157-023-09649-0

Beasley, T. M. (2008). Seemingly unrelated regression (sur) models as a solution to path analytic models with correlated errors. *Multiple Linear Regression Viewpoints*, *34*.

Blackford, J. (2022). *Carbon capture and storage and the marine environment: Impact assessment and assurance monitoring* (Doctoral dissertation, University of Exeter, Exeter, UK). Retrieved from https://hdl.handle.net/10871/126752

Bui, M., Adjiman, C. S., Bardow, A., Anthony, E. J., Boston, A., Brown, S. & Mac Dowell, N. (2018). Carbon capture and storage (ccs): the way forward. *Energy & Environmental Science*, *11*(5), 1062-1176.

Chylek, P., Follandr, C., Klett, J., Wang, M., Hengartner, N., Lesins, G. & Dubey, M. (2022). Annual mean arctic amplification 1970-2020: Observed and simulated by cmip6 climate models. *Geophysical Research Letters*, *49*, e2022GL099371. doi: 10.1029/2022GL099371

Dauginis, A. A. & Brown, L. C. (2021). Recent changes in pan-arctic sea ice, lake ice, and snow-on/off timing. *The Cryosphere*, *15*, 4781–4805.

Diebold, F. & Rudebusch, G. (2022b). Probability assessments of an ice-free arctic: Comparing statistical and climate model projections. *Journal of Econometrics*, *231*, 520–524.

Diebold, F. X., Rudebusch, G. D., Göbel, M., Coulombe, P. G. & Zhang, B. (2022). When will artic sea ice disappear? projections of area, extent, thickness and volume. *Journal of Econometrics*, *236*(30732).

Gholami, R., Raza, A. & Iglauer, S. (2021). Leakage risk assessment of a co2 storage site: A review. *Earth-Science Reviews*, *223*, 103849. Retrieved from https://doi.org/10.1016/j.earscirev.2021.103849 doi: 10.1016/j.earscirev.2021.103849

Goldberger, A. S. (1972). Structural equation methods in the social sciences. *Econometrica*, *40*(6), 979-1001.

International Renewable Energy Agency (IRENA). (2024). *Carbon capture.* https://www.irena.org/Energy-Transition/Technology/Carbon-Capture. (Accessed: 2024-07-01)

Jahn, A., Randall, D. A., Holland, M. M. & Senior, C. A. (2016). Consequences of changes in arctic sea ice cover for the climate. *Journal of Climate*, *29*(16), 5523-5545. Retrieved from https://doi.org/10.1175/JCLI-D-15-0853.1 doi: 10.1175/JCLI-D-15-0853.1

Johannessen, O. M. (2017). Decreasing arctic sea ice mirrors increasing co2 on decadal time scale. *Atmospheric and Oceanic Science Letters*, *1*.

Johnsen, F. M. (2017). *The development of a weighting method for use in life cycle assessments of amine-based post-combustion carbon capture and storage (ccs) in the arctic region* (Doctoral dissertation, Aalborg University, Aalborg, Denmark). doi: 10.5278/vbn.phd.tech.00001

Joreskog, K. G. (1970). A general method for estimating a linear structural equation system.

Kocs, E. A. (2017). The global carbon nation: Status of co2 capture, storage and utilization. *EPJ Web of Conferences*, *148*, 00002. Retrieved from https://doi.org/10.1051/epjconf/201714800002 doi: 10.1051/epjconf/201714800002

Lei, W., Yuan, X., Ting, M. & Li, C. (2016). Predicting summer arctic sea ice concentration intraseasonal variability using a vector autoregressive model. *Journal of Climate*, *29*, 1529–1543.

Lubrano Lavadera, P., Kühn, D., Dando, B., Lecomte, I., Senger, K. & Drottning, Å. (2018). Co2 storage in the high arctic: efficient modelling of pre-stack depth-migrated seismic sections for survey planning. *Geophysical Prospecting*, *66*(6), 1180–1200. Retrieved from https://doi.org/10.1111/1365-2478.12637 doi: 10.1111/1365-2478.12637

Miller, J. I. & Nam, K. (2020). Dating hiatuses: A statistical model of the recent slowdown in global warming and the next one. *Earth System Dynamics*, *11*, 1123–1132. doi: 10.5194/esd-11-1123-2020

Notz, D. & SIMIP, C. (2020). Arctic sea ice in cmip6. *Geophysical Research Letters*, *47*.

Radcliffe, J. W. (2010). *Scenario analysis – iea, blue map.* Energy Research Partnership. (Available at: http://www.iea.org/techno/etp/)

Rogelj, J., Trewin, B., Haustein, K., Canadell, P., Szopa, S., Milinski, S., ... Zickfeld, K. (2021). Summary for policymakers of the working group i contribution to the ipcc sixth assessment report - data for figure spm.10 (v20210809). *NERC EDS Centre for Environmental Data Analysis*.

Rosenblum, E. & Eisenman, I. (2017). A regime shift in arctic sea ice: Increased transverse flow enhances albedo feedback. *Geophysical Research Letters*, *44*(11), 11210–11219.

Saraceno, G., Alqallaf, F. & Agostinelli, C. (2021). *A robust seemingly unrelated regressions for row-wise and cell-wise contamination.*

Sewall, J. O. & Sloan, L. C. (2004). Less ice, less tilt, less chill: The influence of a seasonally ice-free arctic ocean and reduced obliquity on early paleogene climate. *Geology*, *32*, 477-480.

Shen, Z., Duan, A., Li, D. & Li, J. (2021). Assessment and ranking of climate models in arctic sea ice cover simulation: From cmip5 to cmip6. *Journal of Climate*, *34*, 3609–3627.

Stern, N. (2008). The economics of climate change. *American Economic Review*, *98*, 1-37.

Stroeve, J. & Notz, D. (2018). Changing state of arctic sea ice across all seasons," environmental research letters. *Environmental Research Letters*, *13*.

Stroeve, J., Serreze, M., Holland, M., Kay, J., Malanik, J. & Barrett, A. (2012). The arctic's rapidly shrinking sea ice cover: A research synthesis. *Climatic Change*, *110*, 1005-1027.

A CO2 Concentration

Figure 7: Univariate and Bivariate Models For Carbon-Space using 10 seeds (under SSP3 7.0)

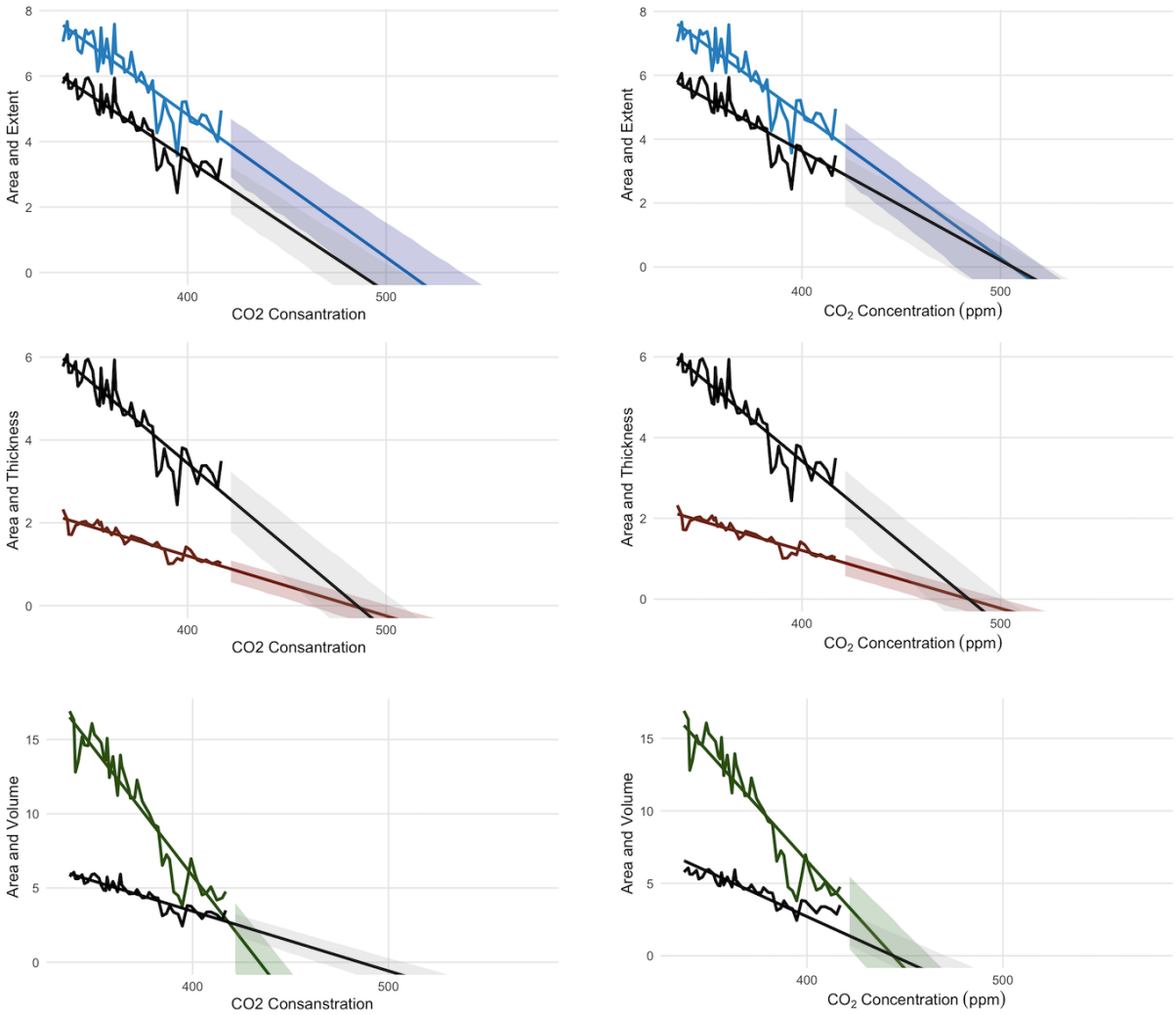

Figure 8: Univariate and Bivariate Models For Time-Space (under SSP3.70)

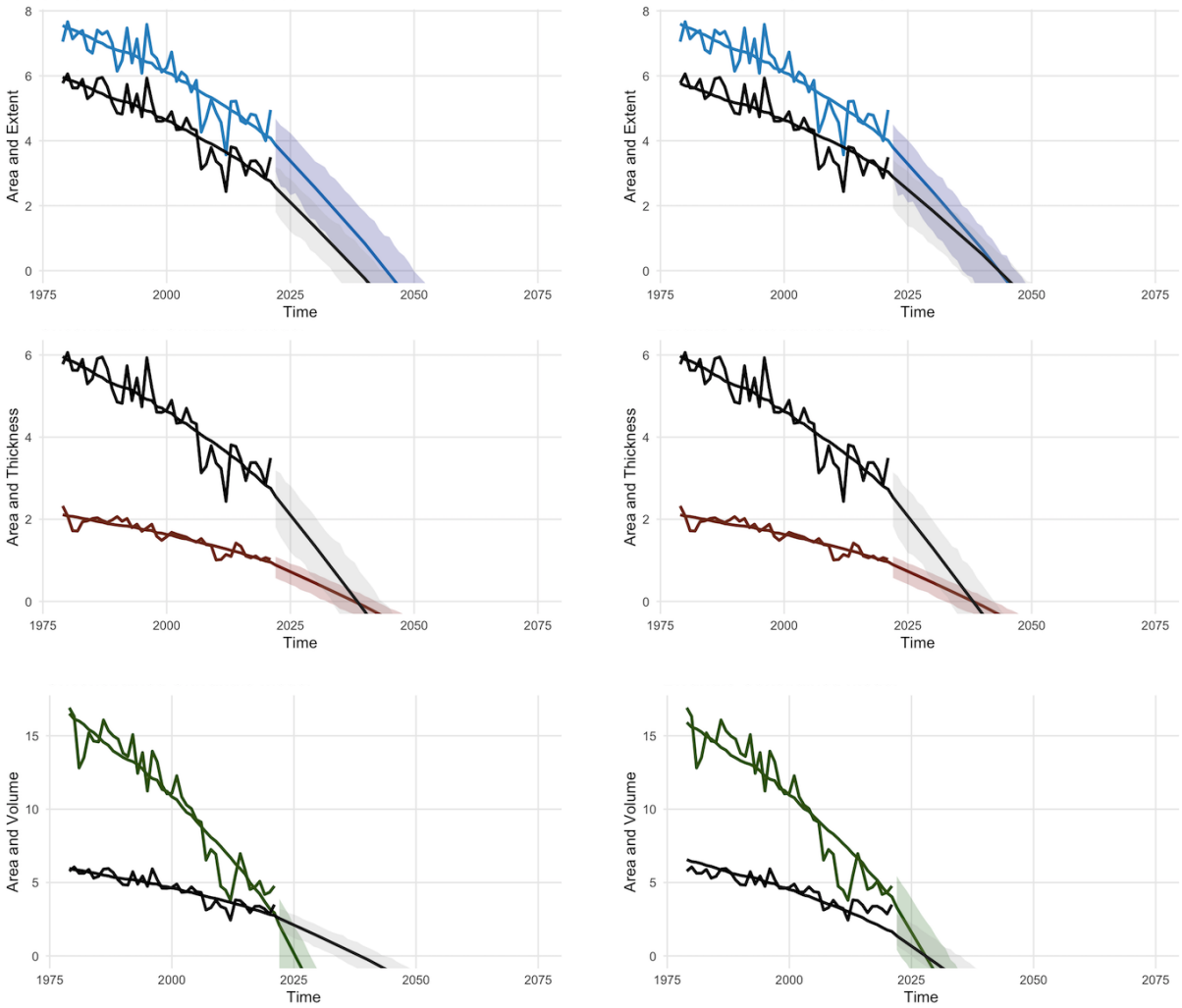

Figure 9: Multivariate Models For Carbon and Time-Space (under SSP3 7.0)

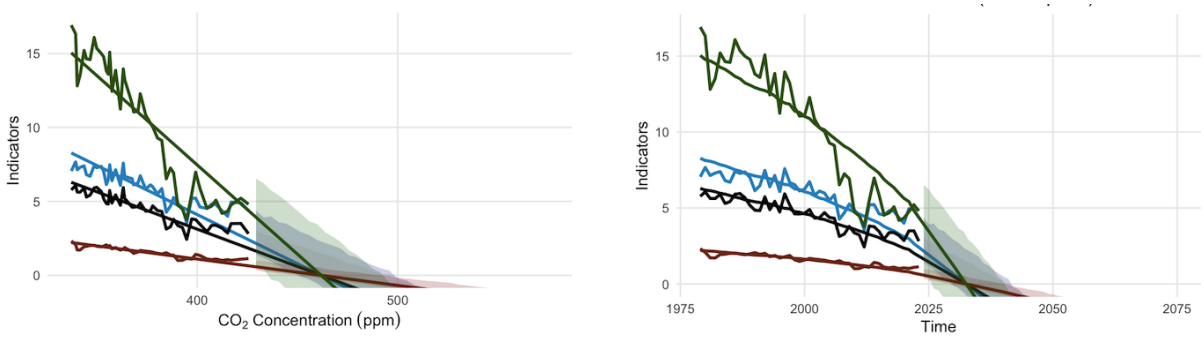

B CO2Emission

Figure 10: Univariate and Bivariate Models Time-Space (Under SSP3.70)

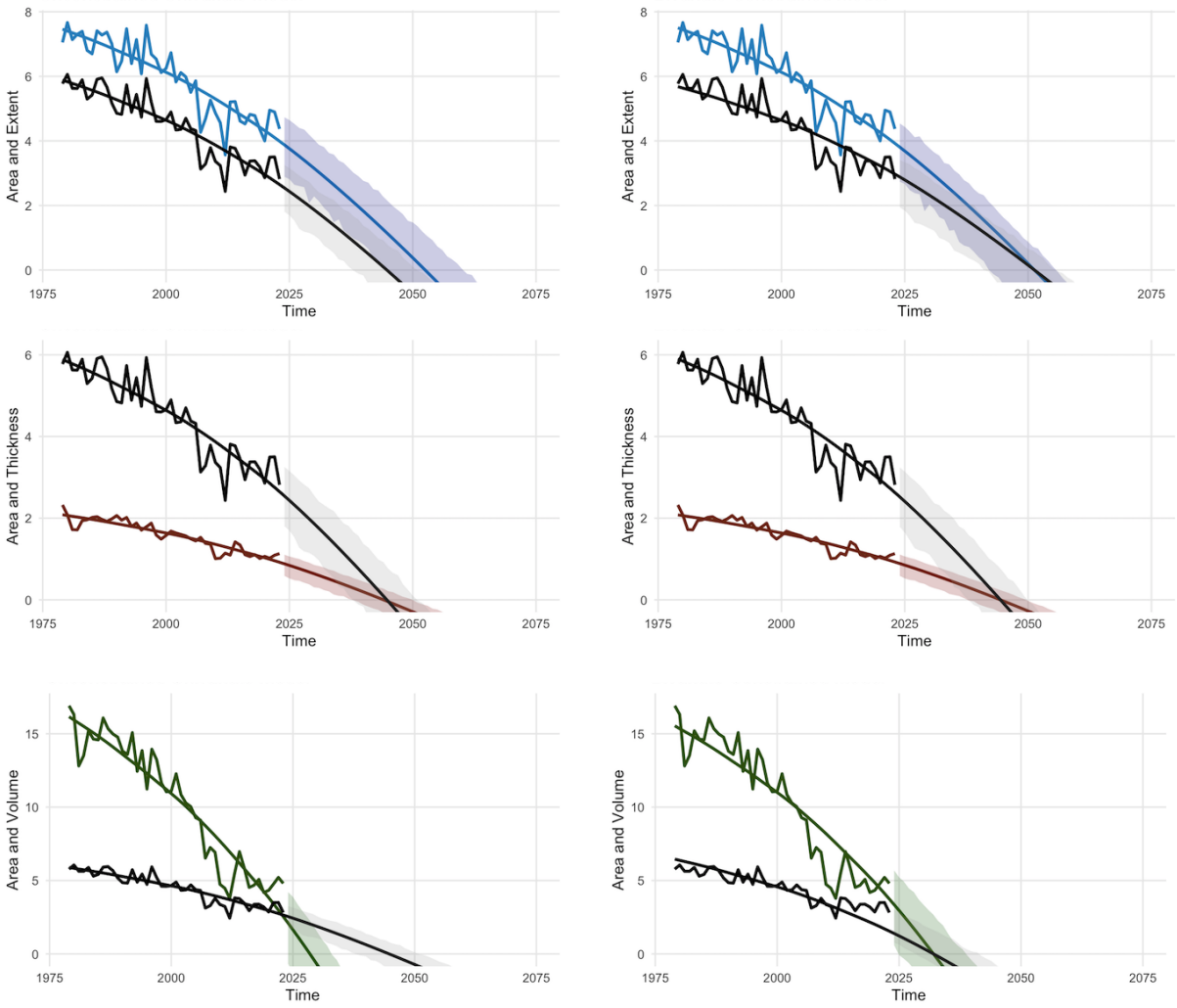

Figure 11: Multivarate Models For Carbon and Time-Space (Under SSP3.70)

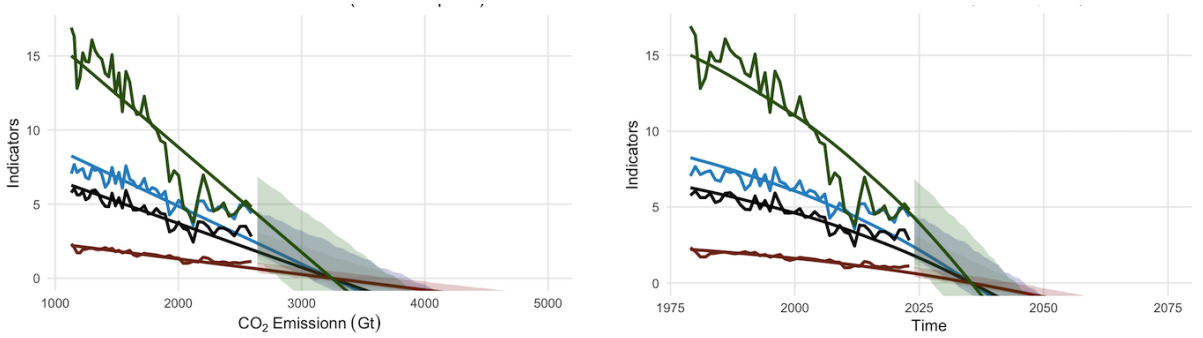

Table 5: September Arctic Sea-Ice Indicators: Linear CO2 Carbon Trend Estimates and Projections (Under SSP3 7.0)

			First IFA		First NIFA (Area)	
Model	$\hat{b}$	R^2	CO2C (ppm)	year	CO2C (ppm)	year
Unconstrained Univariate Models						
Area	−0.0022	0.83	3721	2045	3350	2038
	(0.00015)					
Extent	−0.0024	0.79	4159	2053	NA	NA
	(0.00018)					
Thickness	−0.0008	0.85	3721	2045	NA	NA
	(0.00005)					
Volume	−0.0093	0.90	2888	2029	NA	NA
	(0.00048)					
Constrained Bivariate Models						
SIE+SIA	−0.0019	0.81	4242	2052	3684	2043
	(0.00014)					
SIT+SIA	−0.0022	0.83	3805	2045	3332	2037
	(0.00012)					
SIV+SIA	−0.0034	0.59	3108	2033	2790	2027
	(0.00018)					
Constrained Multivariate Model						
Multivariate	−0.0030	0.73	3275	2036	2946	2030
	(0.00015)					

Table 6: September Arctic Sea-Ice Indicators: Probability Distributions of *SIA* First September NIFA Years

	Mean	**Median**	**Mode**	**SD**	**Skew**	**Kurt**	**5%**	**20%**	**80%**	**90%**
SSP5 8.5										
SIE+SIA	2036	2037	2039	3.75	-0.49	2.89	2029	2033	2039	2042
SIT+SIA	2034	2035	2035	3.07	-0.54	2.89	2028	2032	2037	2038
SIV+SIA	2027	2026	2026	1.93	0.60	2.99	2024	2025	2028	2030
Multi	2030	2030	2029	2.41	0.18	2.89	2026	2028	2032	2034
SSP3 7.0										
SIE+SIA	2037	2037	2038	4.07	-0.42	2.71	2029	2033	2040	2043
SIT+SIA	2034	2035	2036	3.28	-0.50	2.79	2028	2032	2037	2039
SIV+SIA	2027	2026	2026	1.95	0.63	2.99	2024	2025	2028	2030
Multi	2030	2030	2029	2.49	0.19	2.95	2026	2028	2032	2034
SSP2 4.5										
SIE+SIA	2040	2040	2039	4.75	-0.22	2.63	2031	2036	2044	2047
SIT+SIA	2036	2037	2038	3.87	-0.39	2.70	2029	2033	2040	2042
SIV+SIA	2027	2027	2026	2.30	0.66	3.12	2024	2025	2029	2031
Multi	2031	2031	2031	2.90	0.19	2.83	2027	2029	2034	2036
SSP1 2.6										
SIE+SIA	2045	2044	2047	8.00	0.55	3.85	2033	2038	2051	2058
SIT+SIA	2040	2040	2041	5.21	0.066	2.83	2030	2035	2045	2048
SIV+SIA	2028	2027	2026	2.51	0.66	3.10	2024	2025	2030	2032
Multi	2032	2032	2031	3.51	0.27	2.80	2027	2029	2035	2039

C CO2 Emission CCS Scenarios

Figure 12: Univariate and Bivariate Models Time-Space (Under SSP3.70)

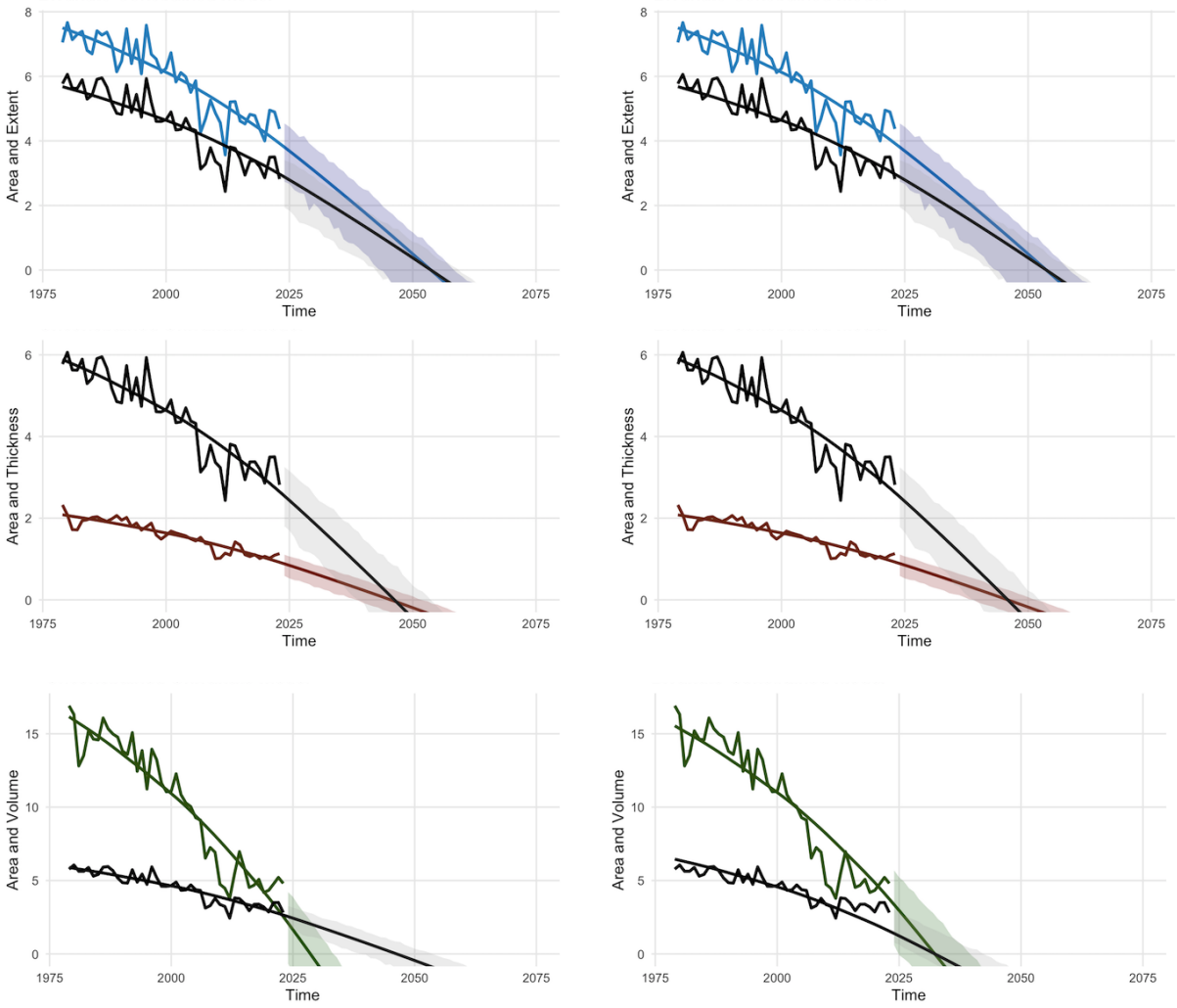

Figure 13: Multivarate Models For Carbon and Time-Space (Under SSP3.70)